

Electronic, magnetic and galvanomagnetic properties of Co-based Heusler alloys: possible states of a half-metallic ferromagnet and spin gapless semiconductor

A. A. Semiannikova^{1*}, Yu. A. Perevozchikova¹, V. Yu Irkhin¹, E. B. Marchenkova¹, P. S. Korenistov¹, and V. V. Marchenkov^{1,2*}

¹ 620108, M.N. Mikheev Institute of Metal Physics, Ekaterinburg, Russia

² 620002, Ural Federal University, Ekaterinburg, Russia

* e-mail: semiannikova@imp.uran.ru, march@imp.uran.ru

Abstract

Parameters of the energy gap and, consequently, electronic, magnetic and galvanomagnetic properties in different X_2YZ Heusler alloys can vary quite strongly. In particular, half-metallic ferromagnets (HMFs) and spin gapless semiconductors (SGSs) with almost 100% spin polarization of charge carriers are promising materials for spintronics. The changes in the electrical, magnetic and galvanomagnetic properties of the Co_2YSi ($Y = Ti, V, Cr, Mn, Fe$) and Co_2MnZ Heusler alloys ($Z = Al, Si, Ga, Ge$) in possible HMF and/or SGS states were followed and their interconnection was established. Significant changes in the values of the magnetization and residual resistivity were found. At the same time, the correlations between the changes in these electronic and magnetic characteristics depending on the number of valence electrons and spin polarization are observed.

Introduction

The motivation is that half-metallic ferromagnets (HMFs) and spin gapless semiconductors (SGSs) are promising materials for spintronics with almost 100% spin polarization of charge carriers. They possess a gap near the Fermi energy for the current carriers with spin down. However, for the opposite spin projection, these materials have a difference: the energy gap absences in HMFs, while it being zero in SGSs Refs. 1, 2.

It is not easy to unambiguously determine the conditions for the occurrence of HMF-states and, especially, SGS in practice. However, the observation of HMF and SGS-states was proposed in materials based on the Co_2YSi ($Y = Fe, Mn$), Mn_2CoAl and $CoFeMnSi$ Heusler alloys and close to 100% spin polarization in Refs. 3-7. The densities of electronic states near the Fermi level E_F change strongly with variation of the Y - and Z -components in the X_2YZ Heusler compounds, which appears in changes in the electronic, magnetic, and optical properties Refs. 8-15. Generally, Y are 3d-transition metals, and Z are elements of the III-V group of the Periodic Table in the stoichiometric formula of Heusler alloys. Therefore, the aim of the work is to follow the changes in the electrical, magnetic and galvanomagnetic properties and to establish their interconnection and basic behavior patterns of the Co_2YSi ($Y = Ti, V, Cr, Mn, Fe$) and Co_2MnZ Heusler alloys ($Z = Si, Al, Ga, Ge$) in the HMF- and/or SGS-states.

Experimental

Polycrystalline Co_2YSi ($Y = Ti, V, Cr, Mn, Fe$) alloys were prepared in an induction furnace in a purified argon atmosphere. Then, the obtained Co_2VSi , Co_2CrSi , and Co_2FeSi ingots were annealed at 1100°C for 3 days and quenched, whereas the Co_2TiSi and Co_2MnSi alloys were annealed at 800°C for 9 days, followed by cooling to the room temperature. Polycrystalline Co_2MnZ ($Z = Al, Si, Ga, Ge$) alloys were prepared by arc melting methods in a purified argon atmosphere and annealed at 800 K during 48 h.

An elemental analysis was carried out by using a FEI Company Quanta 200 scanning electron microscope equipped with an EDAX X-ray microanalysis unit at the Collaborative Access Center «Testing Center of Nanotechnology and Advanced Materials» of the IMP UB RAS. The elemental composition was determined in at least three regions selected at three different points of the sample. The deviation from a stoichiometric composition was revealed to be insignificant in all the samples.

The electrical resistivity was measured by using a standard four-probe method in the temperature range from 0 to 300 K according to Ref. 16. The field dependences of the magnetization $M(H)$ $T = 4.2$ K were measured at in magnetic fields up to 50 kOe. The magnetization was measured using an MPMS-XL-5 SQUID magnetometer. A method for preparing samples and measuring magnetization are described in Ref. 17.

Results and discussion

Fig. 1 shows the X-ray diffraction patterns of Co_2YSi ($Y = \text{Ti, V, Cr, Mn, Fe}$) and Co_2MnZ ($Z = \text{Al, Si, Ga, Ge}$) alloys at room temperature. All alloys are seen to have the structure of the Heusler phase L_{21} , which is evidenced by the presence of Bragg superstructure reflections of the 111 and 200 types. The lattice parameters presented in Tables I and II were determined. The experimental results are comparable with the data given in the literature, e.g. Ref. 18, see Tables I and II.

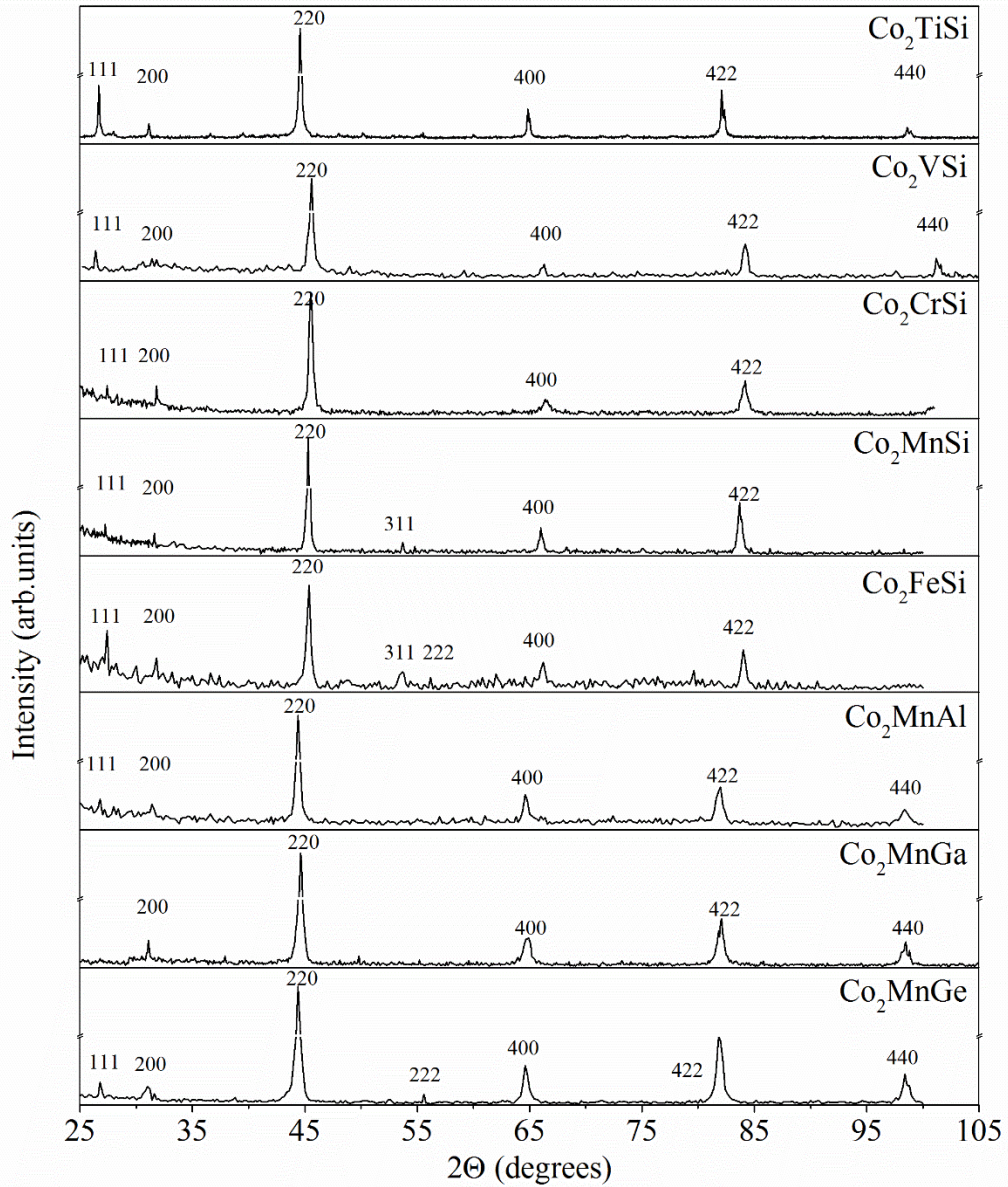


Figure 1 - X-ray diffraction patterns of Co_2MnZ ($Z = \text{Al}, \text{Ga}, \text{Ge}, \text{Sn}$) and Co_2YSi ($Y = \text{Ti}, \text{V}, \text{Cr}, \text{Mn}, \text{Fe}$) alloys

The electrical resistivity was measured in a wide temperature range from 4.2 to 300 K. Figs. 2 and 3 show that the $\rho(T)$ of the Co_2VSi , Co_2CrSi and Co_2MnAl are established to tend to saturation, while the $\rho(T)$ dependences for Co_2TiSi , Co_2FeSi , Co_2MnGa , Co_2MnSi and Co_2MnGe are linear at temperatures above 100 K.

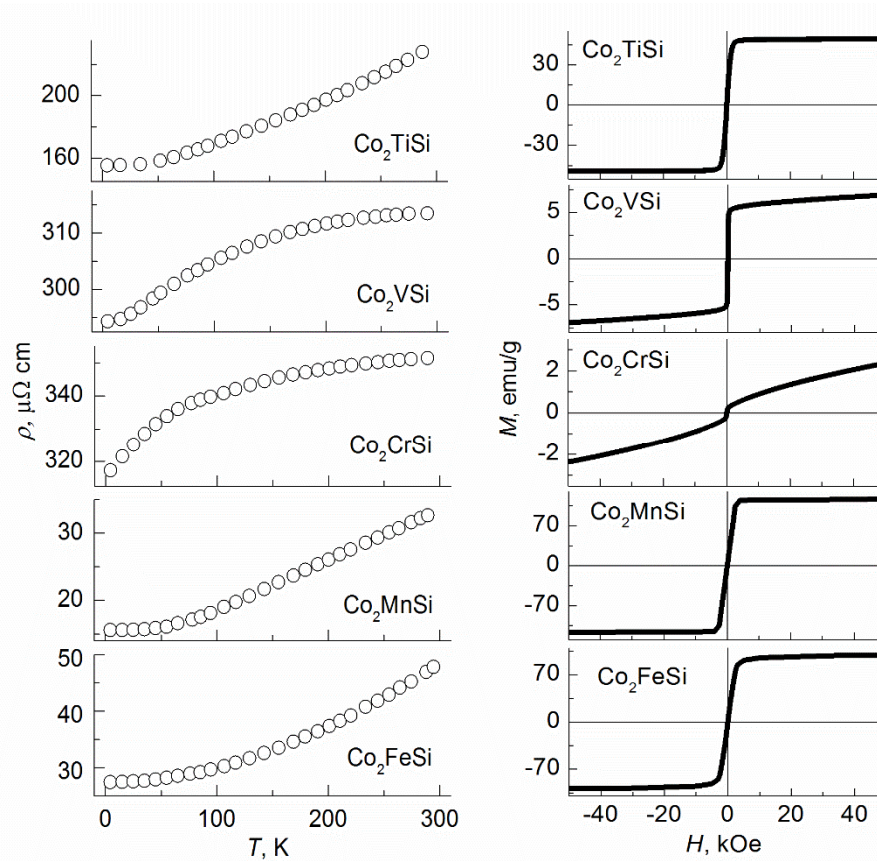


Figure 2— Temperature dependences of the electrical resistivity and field dependences of the magnetization at $T = 4.2$ K for the Co_2YSi system

The residual resistivity ρ_0 was determined at the temperature $T = 4.2$ K for the Co_2YSi

($Y = \text{Ti, V, Cr, Mn, Fe}$) system, Co_2MnAl and Co_2MnSi , the ρ_0 for the Co_2MnGa and Co_2MnGe was found by extrapolation the temperature dependences of resistivity to $T = 4.2$ K.

Tables I and II contain values of the residual resistivity ρ_0 , saturation magnetization M_s ,

lattice parameters, spin polarization of current carriers.

Table I- Number of valence electrons, the experimental lattice parameter, residual resistivity, saturation magnetization and spin polarization for the Co_2YSi system

Compound	z	r_0 , μWcm	M_s , emu/g	P , % Refs. 3, 7, 19, 20	a_{exp} , \AA	a , \AA Ref. 18
Co_2TiSi	26	155	48.8	24	5.747	5.743
Co_2VSi	27	294	5.9	35	5.650	5.657
Co_2CrSi	28	318	1.0	80	5.640	5.647
Co_2MnSi	29	16	114.2	93	5.660	5.645

Co ₂ FeSi	30	27	96.7	57	5.640	5.640
----------------------	----	----	------	----	-------	-------

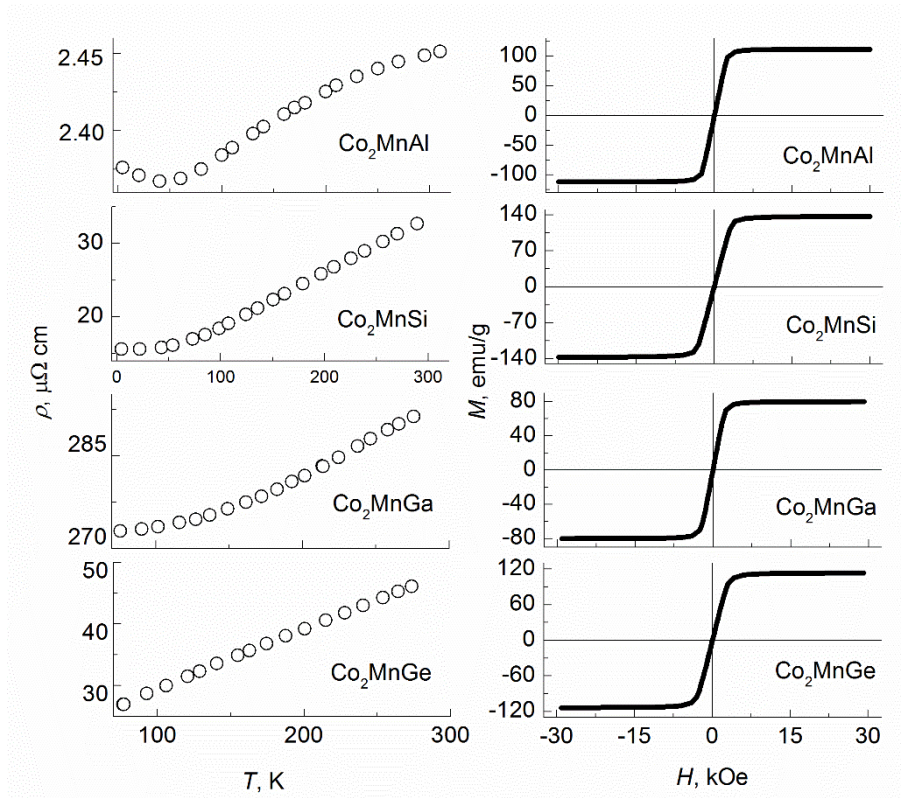


Figure 3 – Temperature dependences of the electrical resistivity and field dependences of the magnetization at $T = 5$ K for the Co_2MnZ system

Figs. 2 and 3 demonstrate that the magnetization curves $M(H)$ have a form characteristic of ordinary ferromagnets. These dependences do not demonstrate rapid saturation for Co_2VSi and Co_2CrSi which seem to be weak itinerant magnets rather than strong half-metallic ferromagnets.

The Co_2VSi , Co_2CrSi and Co_2MnGa alloys demonstrate relatively large residual resistivity ρ_0 varying from 272 to 318 $\mu\Omega \times \text{cm}$, simultaneously, the Co_2VSi and Co_2CrSi possess relatively low values of the saturation magnetization M_s . The occurrence of such peculiarities may indicate unique features near the Fermi level E_F , e.g., the proximity to the SGS-state with a small gap and low activation energy. On the contrary, Co_2MnSi , Co_2FeSi and Co_2MnAl have large M_s and small ρ_0 values, therefore, the HMF-state seems to be observed.

Significant changes in the values of these properties are found. At the same time, the interconnection is observed between the changes in these electronic and magnetic characteristics depending on the number of valence electrons.

Table II – The experimental lattice parameter, residual resistivity, saturation magnetization and spin polarization for the Co_2MnZ system

Compound	r_0 , μWcm	M_s , emu/g	P , % Ref. 21	a_{exp} , Å	a , Å Ref. 18
Co ₂ MnAl	2.4	110.7	65.2	5.765	5.749
Co ₂ MnSi	16	132.2	100	5.660	5.645
Co ₂ MnGa	272	79.9	63.4	5.760	5.767

Co ₂ MnGe	24	108.7	100	5.760	5.749
----------------------	----	-------	-----	-------	-------

Fig. 4 demonstrates temperature dependences of the magnetization at $H = 30$ kOe for the Co₂YSi and Co₂MnZ systems.

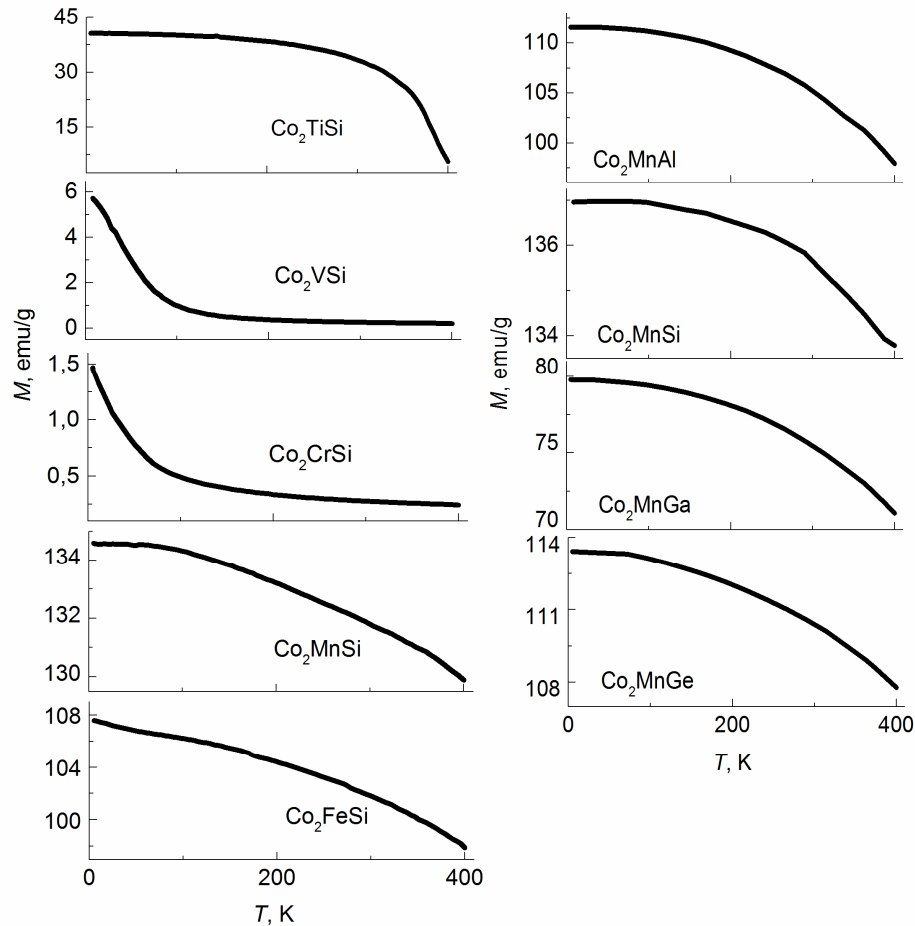


Figure 4 - Temperature dependences of the magnetization at $H = 30$ kOe for the Co₂YSi (on the left) and Co₂MnZ (on the right) systems

Fig. 5 shows the calculated and experimental values of the coefficients of spin polarization of current carriers for the Co₂YSi system taken from Refs. 3, 7, 19, 20 on the number of valence electrons z . It seems very interesting to analyze the behavior of the spin polarization with a change in the number of valence electrons and compare it with the data of the residual resistivity and the saturation magnetization. Fig. 5 shows a good correlation between the experimental data obtained in this work and the coefficient of current carriers spin polarization P from literature data. When the number of valence electrons changes, the spin polarization peaks at $z = 28$ and $z = 29$ for Co₂CrSi and Co₂MnSi.

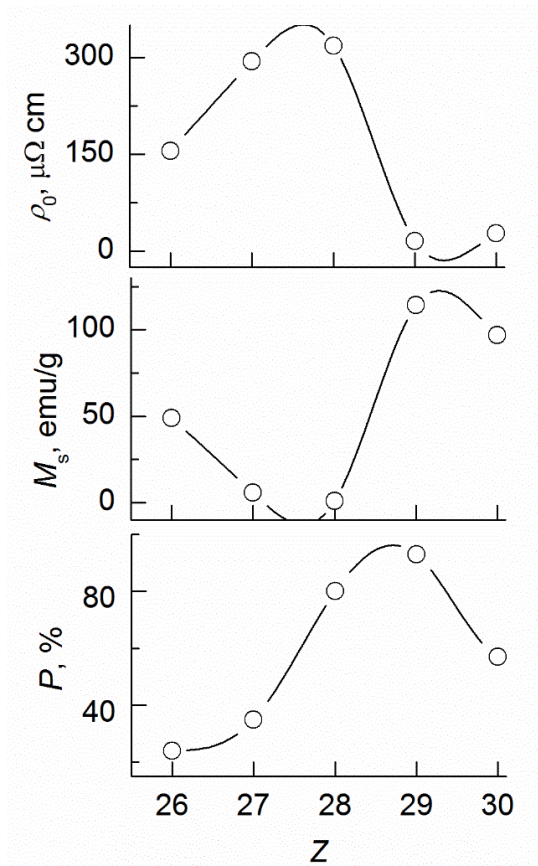


Figure 5 – The correlation with spin polarization for the Co_2YSi system

Fig. 6 presents the correlation between obtained experimental data and the coefficients of current carriers spin polarization for the Co_2MnZ system Ref. 21, when Z-component varies from Al to Ge according to their atomic mass. Thus Z-component variations change considerably atomic potentials and physical properties. Methods for determining spin polarization: VASP + GGA functional Ref. 19, 20, Point Contact Andreev Reflection (PCAR) spectroscopy Ref. 7, Spin resolved ultraviolet-photoemission spectroscopy (SRUPS) Ref. 3, GGA functional Ref. 21.

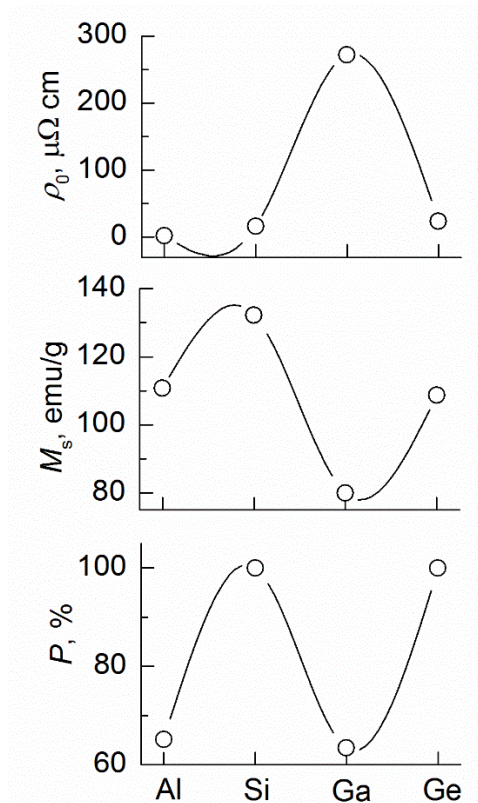


Figure 6 – The correlation with spin polarization for the Co_2MnZ system

A comparison of Figs. 5 and 6 indicates that the correlation is observed between the properties both in the Co_2YSi and Co_2MnZ systems of Heusler alloys. The spin polarization values are consistent with the previously stated assumption that the Co_2MnSi alloy has a high spin polarization, which can be used for choosing promising materials for spintronic devices.

Conclusions

A number of features of electronic and magnetic properties can indicate peculiarities of the electron energy spectrum, i.e. HMF- and/or SGS-states. In some cases, the available experimental techniques do not allow to unambiguously distinguish between these situations.

New information has been obtained on the features of the electronic and magnetic characteristics of the Co_2YSi ($Y = \text{Ti, V, Cr, Mn, Fe}$) and Co_2MnZ ($Z = \text{Al, Si, Ga, Ge}$) Heusler alloys, which may be useful in choosing optimal materials for spintronic devices.

Investigations of magnetization enable one to prove half-metallic nature of ferromagnetism and verify results of band structure calculations.

Acknowledgments

The work was performed within the framework of the state assignment of the Ministry of Science and Higher Education of Russia (the themes “Spin”, No. AAAA-A18-118020290104-2-2 and “Quantum” No. AAAA-A18-118020190095-4) with partial support from the RFBR (projects No. 18-02-00739 and 20-32-90065) and the Government of the Russian Federation (Decree No. 211, Contract No. 02.A03.21.0006).

Data availability

The data that support the findings of this study are available from the corresponding author upon reasonable request.

References

- 1 M. I. Katsnelson, V. Yu. Irkhin, L. Chioncel, A. I. Lichtenstein and R. A. de Groot., *Rev. Mod. Phys.* 80, 315 (2008).
- 2 X. L. Wang, *Phys. Rev. Lett.* 100, 156404 (2008).
- 3 M. Jourdan, J. Minarr, J. Braun, A. Kronenberg, S. Chadov, B. Balke, A. Gloskovskii, M. Kolbe, H. J. Elmers, G. Schonhense, H. Ebert, C. Felser, and M. Klaui, *Nat. Commun.* 5, 3974 (2014).
- 4 S. Ouardi, G. H. Fecher, C. Felser, and J. Kübler, *Phys. Rev. Lett.* 110, 100401 (2013).
- 5 L. Bainsla, A. I. Mallick, M. M. Raja, A. K. Nigam, B. S. D. Ch. S. Varaprasad, Y. K. Takahashi, Aftab Alam, K. G. Suresh, and K. Hono, *Phys. Rev. B* 91, 104408 (2015).
- 6 V.V. Marchenkov, N.I. Kourov, and V.Yu. Irkhin, *Phys. Met. Metallogr.* 119, 64 (2018)
- 7 L. Makinistian, M.M. Faiz, R.P. Panguluri, B. Balke, S. Wurmehl, C. Felser, E.A. Albanesi, A. G. Petukhov, and B. Nadgorny, *Phys. Rev. B* 87, 220402 (2013)
- 8 V. V. Marchenkov, Yu. A. Perevozchikova, N. I. Kourov, V. Yu. Irkhin, M. Eisterer, and T. Gao, *J. Magn. Magn. Mat.* 459, 211 (2018).
- 9 N. I. Kourov, V. V. Marchenkov, K. A. Belozeroва, and H. W. Weber, *JETP* 118, 426 (2014).
- 10 N. I. Kourov, V. V. Marchenkov, K. A. Belozeroва, and H. W. Weber, *JETP* 121 (5), 844 (2015).
- 11 N. I. Kourov, V. V. Marchenkov, A. V. Korolev, A. V. Lukoyanov, A. A. Shirokov, and Yu. A. Perevozchikova, *Mater. Res. Express* 4, 116102 (2017).
- 12 K. A. Fomina, V. V. Marchenkov, E. I. Shreder and H. W. Weber, *SSP* 168, 545 (2011).
- 13 N. I. Kourov, V. V. Marchenkov, A. V. Korolev, K. A. Belozeroва, H. W. Weber. *Curr. Appl. Phys.* 15, 839 (2015).

- 14 Yu. A. Perevozchikova, A. A. Semiannikova, A. N. Domozhirova, P. B. Terentyev, E. B. Marchenkova, E. I. Patrakov, M. Eisterer, P.S. Korenistov, and V.V. Marchenkov, *Low Temp. Phys.* 45, 789 (2019).
- 15 Yu. A. Perevozchikova, A. A. Semiannikova, P. B. Terentyev, M. Eisterer, P. S. Korenistov, and V. V. Marchenkov, *Journal of Physics: Conf. Series* 1389, 012110 (2019).
- 16 A. N. Cherepanov, V. V. Marchenkov, V. E. Startsev, N. V. Volkenshtein, and M. Glin'ski, *J. Low Temp. Phys.* 80, 135 (1990).
- 17 S. M. Emelyanova, N. G. Bebenin, V. P. Dyakina, V. V. Chistyakov, T. V. Dyachkova, A. P. Tyutyunnik, R. L. Wang, C. P. Yang, F. Sauerzopf, and V. V. Marchenkov, *Phys. Met. Metallogr.* 119, 121 (2018).
- 18 H. C. Kandpal, G. H. Fecher, C. Felser, *J. Phys. D: Appl. Phys.*, 40(6), 1507 (2007).
- 19 C. Xing-Qiu, R. Podloucky, and P. Rogl, *J. Appl. Phys.* 100, 113901(2006).
- 20 S. V. Faleev, Y. Ferrante, J. Jeong, M. G. Samant, B. Jones, and S. S. P. Parkin, *Phys. Rev.* 1, 024402 (2017).
- 21 A. Candan, G. Ugur, Z. Charifi, H. Baaziz, M. R. Ellialtioglu, *J. Alloys Compd.* 560, 215 (2013).